Resonant Body Transistors in IBM's 32nm SOI CMOS Technology

R. Marathe, W. Wang, Z. Mahmood, L. Daniel, D. Weinstein
Massachusetts Institute of Technology, Cambridge, MA
Email: dana@mtl.mit.edu, Tel: (617) 253-8930

This work presents an unreleased CMOS-integrated MEMS resonators fabricated at the transistor level of IBM's 32SOI technology and realized without the need for any post-processing or packaging. These Resonant Body Transistors (RBTs) are driven capacitively and sensed piezoresistively using an n-channel Field Effect Transistor (nFET). Acoustic Bragg Reflectors (ABRs) are used to localize acoustic vibrations in these resonators completely buried in the CMOS stack and surrounded by low-k dielectric. Experimental results from the first generation hybrid CMOS-MEMS show RBTs operating at 11.1-11.5 GHz with footprints < 5µm × 3µm. The response of active resonators is shown to contrast with passive resonators showing no discernible peak. Comparative behavior of devices with design variations is used to demonstrate the effect of ABRs on spurious mode suppression. Temperature stability and TCF compensation due to complimentary materials in the CMOS stack are experimentally verified.

INTRODUCTION

RF MEMS resonators offer an attractive alternative to their counterparts such as LC tanks and SAW devices owing to their high Q, small footprint, and low power operation. Furthermore, Si-based resonators offer designers the possibility of embedding these resonators directly within the CMOS stack [1]. This leads to reduced parasitics from on and off-chip routing for high frequency operation, smaller size and weight, and decreased power consumption by alleviating constraints for impedance matching networks [2,3].

The authors have previously demonstrated Resonant Body Transistors (RBTs) [4,5] with internal dielectric drive and Field Effect Transistor (FET) sensing up to 37 GHz. FET-sensing has thus been shown to reach orders of magnitude higher frequencies than possible with passive resonators due to the active amplification of the resonance signal before the presence of parasitics.

RBTS IN IBM 32NM SOI PROCESS

A schematic of one variation of the 32nm RBT is shown in Fig. 1. Due to material restrictions in CMOS, electrostatic transduction is considered to take advantage of the gate stack. devices are driven electrostatically and acoustically sensed using a FET. Structurally, the drive capacitor consists of PolySi gate material and a p or n-doped SCS device layer acting as capacitor plates with the SiON gate dielectric between them [6]. On the sense side, a foundry-provided body-contacted nFET is modified to incorporate it within the resonant cavity along with the capacitor on the same device layer.

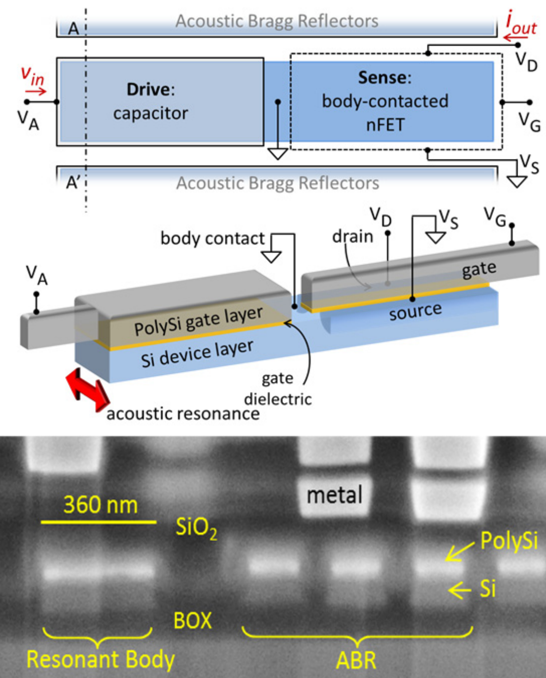

Fig. 1: Schematic and SEM of CMOS-MEMS Resonant Body Transistor. The resonant cavity is composed of the Si device layer and Poly gate layer, with Si Acoustic Bragg Reflectors (ABRs) adjacent to the resonant cavity.

In operation, the FET is biased into saturation while grounding the body separately from the source to reduce feed-through. A small AC voltage is superimposed on top of a DC bias to squeeze the capacitor dielectric which translates into longitudinal strain through the Poisson effect. At resonance, the strain in the nFET channel on the sensing side modulates carrier mobility, resulting in an AC drain current. In Si piezoresistive sensing provides >10× boost in sensing as compared to capacitive sensing. Furthermore, the decoupling of the drive and sense mechanisms reduces the feed-through parasitics.

In this design, Si/SiO_2 was chosen as the material combination for ABRs as these materials occur in the easily patterned Shallow Trench Isolation (STI) structures offered in this technology. The acoustic impedance mismatch between Si and SiO_2 is $Z_{rel} = Z_{Si} / Z_{SiO2} \sim 1.47$ and the resultant reflectivity achieved using 7 pairs of ABRs is $R \sim 99.4\%$ based on 1D analysis [7].

EXPERIMENTAL RESULTS

The frequency response of the input to output transconductance of an nFET-ncap device is shown in Fig. 2. The device shows a resonance frequency of 11.1

978-1-4673-2691-9/12/$31.00 ©2012 IEEE

GHz with a Q~17 extracted from FWHM. The amplitude of the resonance peak changes with the actuation gate voltage V_A verifying the mechanical nature of the resonance peak. Similarly, a smaller front gate voltage V_G results in a smaller drain current I_D.

Fig. 3 shows the frequency and phase response of pcap-nFET device designed on the same die. This device is driven with a p-doped capacitor instead of an n-doped capacitor and demonstrates a resonance frequency of 11.54 GHz with Q~24 with an improved feedthrough over the ncap-nFET device.

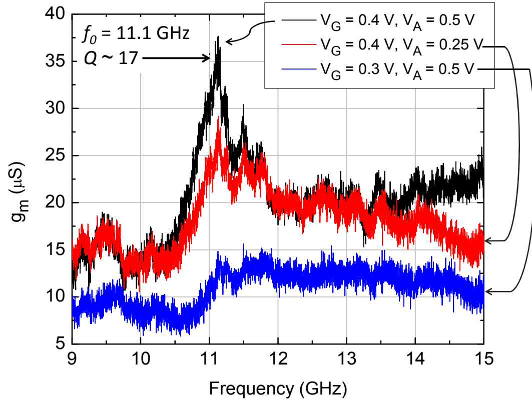

Fig. 2: Frequency response of an nFET-ncap resonator showing a resonance frequency of 11.1 GHz, Q~17. The back gate voltage V_A modulates the gain at resonance verifying the mechanical nature of the resonance peak.

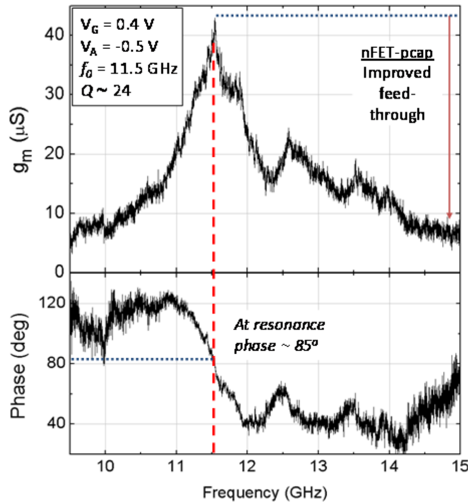

Fig. 3: Frequency response nFET-pcap with improved feed-through relative to the nFET-ncap device.

THERMAL DEPENDENCE

CMOS RBTs were measured between 300K and 380K to extract the temperature dependence. Due to the presence of spurious modes from CMP-fill metal layers above the device, simple Lorentzian fitting to the resonance peak was not sufficient for accurate measurement of the temperature coefficient of frequency (TCF). Fig. 4 shows the TCF of an nFET-ncap RBT extracted using a rational transfer function $H(s) = \sum_{k=1}^{\kappa} R_k/(s - a_k) + D$.

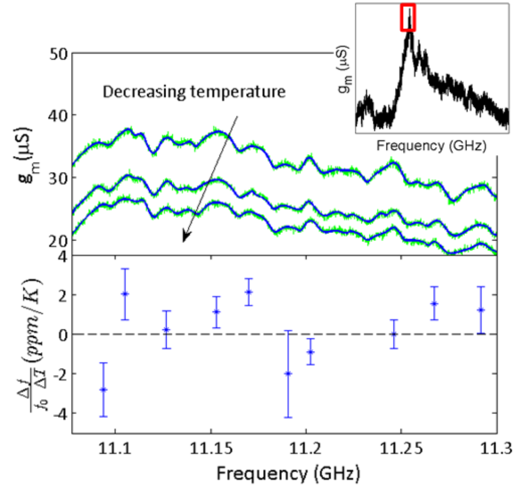

Fig. 4: Zooming in around the measured resonance peak (inset) shows multiple spurious modes that make up the peak. Plot compares measured values of the transconductance and data fitted using rational transfer functions. TCF with error bars plotted against frequency.

Two different families of poles were observed- those showing positive TCF indicating oxide-compensated modes and those with negative TCF showing Si-dominated modes. The complimentary TCF of Si/SiO2 in the CMOS stack in these unreleased resonators provides the opportunity to engineer the TCF of the resonance peak in future designs to either obtain a high TCF for design of temperature sensors or for a low TCF for oscillators and filters.

CONCLUSION

These devices mark the first unreleased resonators to be integrated in an FEOL CMOS process, enabling high frequency operation with small footprint, high, yield, and no post-processing or packaging. Current efforts include the incorporation of Deep Trench Capacitors available in the IBM SOI processes for improved transduction efficiency, reduction in spurious modes, and higher quality factors.

1 R. Marathe, W. Wang, D. Weinstein, *IEEE Micro Electro Mechanical Systems (MEMS),* 729-732 (2012)

2 G. K. Fedder, R. T. Howe, Tsu-Jae King Liu, E.P. Quevy, *Proceedings of the IEEE* , **96**(2), 306-322, (2008)

3 F. H. Xie, L. Erdmann, X. Zhu, K. Gabriel, G.K. Fedder, *J. Microelectromech. Syst.* **11**(2), 93-101 (2002)

4 D. Weinstein, S.A. Bhave, *Nano Letters* **10** (4), 1234-1237 (2010)

5 D. Weinstein, S.A. Bhave, *Hilton Head*, 459-462 (2010)

6 S. S. Iyer, G. Freeman, et. al., *IBM Journal of Research and Development* , **55**(3), 5:1-5:14 (2011)

7 W. Wang, D. Weinstein, *Freq. Control Symp*, 1-6 (2011)